

# Broadband homonuclear chemical shift correlation at high MAS frequencies: a study of tanh/tan adiabatic RF pulse schemes without $^1\text{H}$ decoupling during mixing

Kerstin Riedel · Christian Herbst · Jörg Leppert ·  
Oliver Ohlenschläger · Matthias Görlach ·  
Ramadurai Ramachandran

Received: 3 July 2006 / Accepted: 11 December 2006 / Published online: 8 February 2007  
© Springer Science+Business Media B.V. 2007

**Abstract** At high magic angle spinning (MAS) frequencies the potential of tanh/tan adiabatic RF pulse schemes for  $^{13}\text{C}$  chemical shift correlation without  $^1\text{H}$  decoupling during mixing has been evaluated. It is shown via numerical simulations that a continuous train of adiabatic  $^{13}\text{C}$  inversion pulses applied at high RF field strengths leads to efficient broadband heteronuclear decoupling. It is demonstrated that this can be exploited effectively for generating through-bond and through-space, including double-quantum, correlation spectra of biological systems at high magnetic fields and spinning speeds with no  $^1\text{H}$  decoupling applied during the mixing period. Experiments carried out on a polycrystalline sample of histidine clearly suggest that an improved signal to noise ratio can be realised by eliminating  $^1\text{H}$  decoupling during mixing.

**Keywords** Adiabatic inversion pulses · Chemical shift correlation · MAS · Solid state NMR

## Introduction

Magic angle spinning (MAS) solid state NMR has emerged as a powerful tool for structural studies of biological systems (Thompson 2002; McDermott 2004). A variety of RF pulse schemes for generating dipolar and scalar couplings mediated chemical shift correla-

tion spectra in rotating solids have been reported to achieve resonance assignments and to extract distance and torsion angle constraints from isotopically labelled peptides/proteins and nucleic acids (Bennett et al. 1994; Griffin 1998; Dusold and Sebald 2000; Baldus 2002). Most of the MAS solid state NMR studies of biological systems till date have been carried out with RF pulse schemes based on rectangular pulses. However, experimental imperfections such as  $H_1$  inhomogeneities and resonance offsets can significantly impair the efficacy of sequences based on such pulses. Although these difficulties can be overcome to some extent by using composite pulses and RF phase cycling procedures, in some situations it may not be possible at all to effectively employ pulse schemes based on rectangular RF pulses. For example, the RF field strength requirement for  $RN_n^v$  and  $CN_n^v$  symmetry-based sequences (Carravetta et al. 2000; Brinkmann and Levitt 2001; Levitt 2002) using rectangular RF pulses is related to the spinning speed and this may, at certain spinning speed regimes, lead to the required RF field strength becoming either too large, that may be beyond the hardware limits, or too small, which may affect the performance of the sequence over a large bandwidth. Taking into account all these factors and the fact that many of the MAS solid state NMR pulse schemes employed in structural studies of biological systems are based on  $180^\circ$  pulses, we have been examining in recent years the possibilities for implementing MAS solid state NMR pulse sequences using suitable amplitude and frequency/phase modulated adiabatic inversion pulses instead of conventional rectangular pulses (Heise et al. 2002; Leppert et al. 2002, 2004a; Riedel et al. 2004a, b; Herbst 2006a). Among the different modulation functions proposed for generating

K. Riedel · C. Herbst · J. Leppert · O. Ohlenschläger ·  
M. Görlach · R. Ramachandran (✉)  
Research Group Molecular Biophysics/NMR Spectroscopy,  
Leibniz Institute for Age Research, Fritz Lipmann Institute,  
07745 Jena, Germany  
e-mail: raman@fli-leibniz.de

adiabatic pulses, the tanh/tan pulse (Hwang et al. 1998) constructed from the following adiabatic half passage and its time reversed half passage,

$$\omega_1(t) = \omega_{1(\max)} \tanh(\xi 2t/T_p)$$

$$\Delta\omega(t) = \Delta\omega_{\max}[\tan(\kappa(1 - 2t/T_p))]/\tan(\kappa),$$

with  $0 \leq t \leq T_p/2$ , has been found to be very time efficient. Employing such adiabatic pulse based RF schemes, hetero- and homonuclear chemical shift correlation (Leppert et al. 2004b, c; Riedel 2004; Riedel et al. 2005), including double-quantum NMR (Riedel et al. 2006a, b), experiments have been successfully carried out at moderate spinning frequencies using moderate RF field strengths. However, it has been observed that in situations where inversion pulses of very short duration may be needed, e.g. at very high spinning speeds, the RF power requirements for obtaining satisfactory response from pulse schemes based on adiabatic inversion pulses could become very high. Since the generation of  $^{13}\text{C}$ – $^{13}\text{C}$  dipolar/scalar couplings mediated chemical shift correlation spectra requires effective heteronuclear decoupling during mixing,  $^1\text{H}$  decoupling during the mixing period is commonly employed. However, substantial signal loss due to the interference between the recoupling and decoupling RF fields can arise where sufficient mismatch (~3:1) between the decoupling and recoupling RF field strengths can not be achieved (Bennett et al. 1998). This can be avoided, in principle, by two different approaches. The first approach involves minimising, where possible, the recoupling RF field strength employed by tailoring the frequency and amplitude modulation profiles of the inversion pulses as per experimental requirements such as the spinning speed, inversion bandwidth and the extent of  $H_1$  inhomogeneity compensation needed (Herbst et al. 2006b; Riedel et al. 2006b). The second and more elegant approach involves the design of suitable RF pulse schemes so that  $^1\text{H}$  decoupling during the mixing period is not required at all (Hughes et al. 2004; Marin-Montesinos et al. 2005; De Paepe et al. 2006; Mou et al. 2006). For example, if the RF pulse scheme used during the mixing period of a homonuclear  $^{13}\text{C}$  dipolar chemical shift correlation experiment can recouple not only the  $^{13}\text{C}$ 's but also simultaneously decouple the  $^1\text{H}$  spins, then such RF pulse schemes can be effectively used for obtaining correlation spectra without  $^1\text{H}$  decoupling during mixing. Recent  $^{13}\text{C}$  MAS NMR studies carried out at moderate spinning speeds have shown that it is possible to achieve heteronuclear decoupling by application of a continuous train of short adiabatic  $^1\text{H}$

inversion pulses (Leppert et al. 2004d) and in particular via  $CN_n^v$  symmetry-based adiabatic RF pulse schemes (Riedel et al. 2004a, 2006c). Motivated by these considerations, we have examined here the requirements for achieving efficient broadband heteronuclear decoupling at high spinning speeds via  $^{13}\text{C}$  tanh/tan adiabatic mixing schemes and, hence, the possibilities for generating through-space and through-bond chemical shift correlation spectra without  $^1\text{H}$  decoupling during mixing.

## Experimental and numerical procedures

The RF pulse sequence employed for generating through-space and through-bond  $^{13}\text{C}$  correlation spectra with single-quantum chemical shift evolutions in both the dimensions is shown in Fig. 1a and the pulse scheme for obtaining DQ dipolar chemical shift correlation spectra is given in Fig. 1b. Dipolar correlation spectra were generated essentially by applying one adiabatic inversion pulse at the center of each rotor period during the mixing periods (Heise et al. 2002; Leppert et al. 2003; Riedel et al. 2004b, 2006a, b). In the single-quantum dipolar correlation experiment the adiabatic inversion pulses were phase cycled as per dipolar recoupling schemes such as  $R6_6^2R6_6^{-2}$  (Brinkmann et al. 2002). As in our recent investigations (Riedel et al. 2006a, b), simple phasing schemes such as m4 and m8 (Levitt et al. 1983) were used in the DQ experiment. Through-bond correlation spectra were generated via  $RN_n^v$  and  $CN_n^v$  symmetry-based adiabatic mixing sequences (Carravetta et al. 2000; Brinkmann and Levitt 2001; Levitt 2002). Experiments involving single-quantum chemical shift evolution in both the dimensions were generated via longitudinal magnetisation exchange (Fig. 1a). In Scheme 1b, the transverse magnetisation components created after cross-polarisation, e.g.  $I_{1y}$ , evolve under the ZQ dipolar Hamiltonian created by the recoupling sequence. This leads to the creation of anti-phase coherences, e.g.  $I_{1x}I_{2z}$  and these are converted into DQ coherences by the application of a  $\pi/2$  pulse. Similarly, anti-phase coherences, e.g.  $I_{1x}I_{2z}$ , created by the application of a  $\pi/2$  pulse on DQ coherences, are converted back into observable single quantum coherences, e.g.  $I_{1y}$ , by the ZQ dipolar Hamiltonian. Standard phase cycling procedures were employed to select the desired coherence transfer pathway and phase sensitive 2D spectra were generated via the SHR method (States et al. 1982). Experiments were carried out at room temperature with an undiluted  $^{13}\text{C}$  labelled sample of histidine at a spinning speed of 25 kHz on a 500 MHz wide-bore

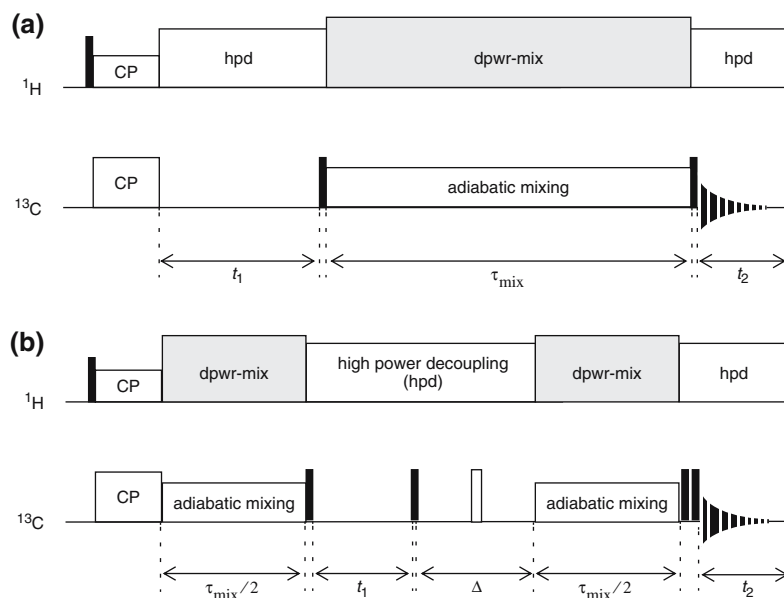


**Fig. 1** RF pulse schemes with adiabatic mixing for generating  $^{13}\text{C}$  chemical shift correlation data in rotating solids. The  $^1\text{H}$  decoupling RF field strength during mixing (dpwr-mix) is set either to zero or to a high value depending on the nature of the experiment carried out. Open and filled rectangles represent  $180^\circ$  and  $90^\circ$  pulses, respectively. Scheme (a)

(Leppert et al. 2003, 2004a), was used for obtaining single-quantum dipolar and scalar coupling mediated chemical shift correlation spectra via longitudinal magnetisation exchange. Scheme (b) (Riedel et al. 2006a, b), was employed for obtaining double-quantum NMR correlation spectra. Further details are given in the text

Varian <sup>UNITY</sup>INOVA solid state NMR spectrometer equipped with a 3.2 mm Chemagnetics triple resonance probe and waveform generators for pulse shaping. The frequency sweep is implemented in the spectrometer hardware as a phase modulation,  $\phi(t) = \int \Delta\omega(t)dt$ . Cross-polarisation under Hartmann–Hahn matching condition was employed and all spectra were collected under TPPM (Bennett et al. 1995) high power decoupling (hpd) in  $t_1$  and  $t_2$  dimensions. Spectra were acquired without or with  $^1\text{H}$  decoupling during mixing using appropriate  $^{13}\text{C}$  RF field strength for adiabatic mixing. The delay  $\Delta$  in Scheme 1b is adjusted such that the total duration ( $\Delta + t_1$ ) always corresponds to an integral number of rotor periods. Tanh/tan adiabatic pulses with  $R$  (representing the product of the pulse-width and  $\Delta\omega_{\text{max}}$ ),  $\tan \kappa$  and  $\zeta$  values of 60, 20 and 10, respectively, as used in many of our recent studies, were uniformly employed in all the investigations. Other details are given in the figure captions.

Numerical simulations were carried out using the SIMPSON program (Bak et al. 2000) at a Zeeman field strength of 11.7 T and neglecting CSAs and resonance offsets, unless mentioned otherwise. Adiabatic inversion pulses of appropriate durations and phases, as determined by the mixing scheme and spinning speed, were used. These pulses were divided into 100 slices of equal duration in the calculations.

## Results and discussion

Considering CH and CH<sub>2</sub> spin systems, the efficacy of heteronuclear decoupling under adiabatic  $^{13}\text{C}$  mixing sequences employed for generating single-quantum or double-quantum correlation data was evaluated via numerical simulations. Starting with either longitudinal or transverse  $^{13}\text{C}$  magnetisation, the magnitude of the relevant magnetisation component was monitored periodically with the rate of sampling determined by the mixing scheme. Representative results from these numerical simulations are shown in Fig. 2. The efficacy of different adiabatic mixing sequences were assessed as a function of the RF field strength and  $^{13}\text{C}$  resonance offset. When the effects of heteronuclear couplings are eliminated during the application of the  $^{13}\text{C}$  adiabatic mixing sequences, the amplitude of the observed magnetisation component will exhibit minimal variations or oscillations as a function of the mixing time. Figure 2 shows the performance seen with mixing schemes used in generating single-quantum dipolar (a1–a6), single-quantum scalar (b1–b3) and double-quantum dipolar chemical shift correlation data (c1–c6). Starting with  $^{13}\text{C}$   $I_z$  magnetisation, the  $\text{R}6_6^2$   $\text{R}6_6^{-2}$  symmetry-based mixing scheme reported by Brinkmann et al. (2002) was employed in a1–a6. This involves the application of one inversion pulse per

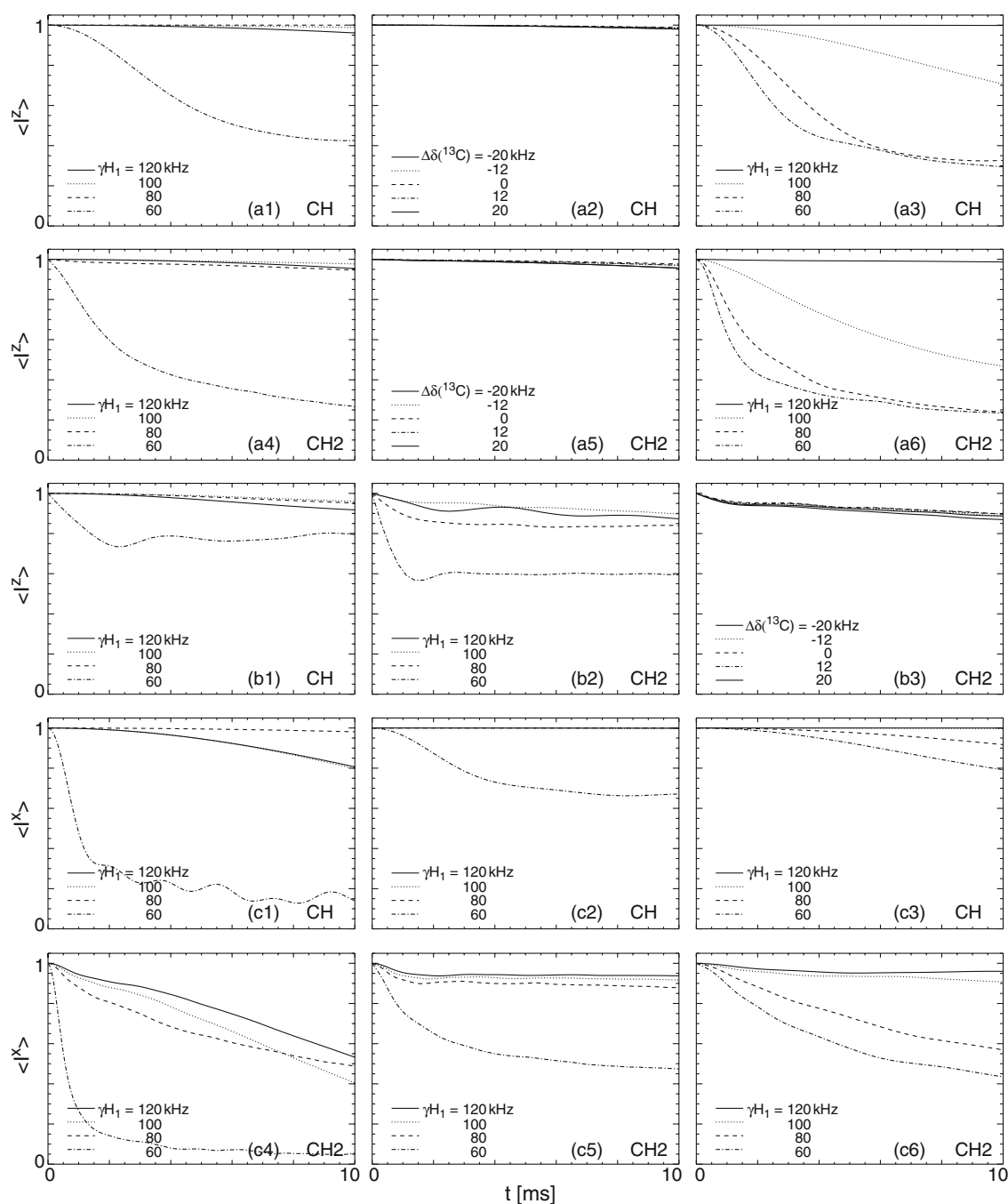


**Fig. 2** Simulations depicting the magnitude of the relevant  $^{13}\text{C}$  magnetisation (either longitudinal or transverse) in CH and CH2 spin systems and as a function of the  $^{13}\text{C}$  RF field strength, resonance offset and adiabatic mixing time. (a1–a6) Single-quantum dipolar mixing,  $\text{R6}_6^2\text{R6}_6^{-2}$  phasing scheme, (b1–b3) single-quantum scalar mixing,  $\text{R32}_{28}^3$  phasing scheme, (c1–c6) double-quantum dipolar mixing, m4 (c1, c4), m8 (c2, c5) and m16 (c3, c6) phasing schemes. Plots were generated at

spinning speeds of 25 kHz (a1, a2, a4, a5, b1–b3, c1, c2, c4, c5) and 40 kHz (a3, a6, c3, c6). Simulations as functions of the  $^{13}\text{C}$  resonance offset were carried out employing a  $^{13}\text{C}$  RF field strength of 100 kHz. Dipolar coupling strengths  $D_{\text{CH}} = 23.3$  kHz and  $D_{\text{HH}} = 21.2$  kHz were used. The powder averaging pattern was based on 256  $[\alpha, \beta]$  orientations selected using the REPULSION scheme (Bak and Nielsen 1997) in combination with 16  $\gamma$  angles

rotor period. Spinning speeds of 25 kHz (a1, a2, a4, a5) and 40 kHz (a3, a6) were used in the simulations. The symmetry-based mixing scheme  $\text{R32}_{28}^3$  with tanh/tan

pulses of 35  $\mu\text{s}$  duration was employed in b1–b3 at a spinning speed of 25 kHz, starting with  $^{13}\text{C}$   $I_z$  magnetisation. Starting with  $^{13}\text{C}$   $I_x$  magnetisation, c1–c6

were generated as a function of the RF field strength with m4 (c1, c4,  $\nu_r = 25$  kHz), m8 (c2, c5,  $\nu_r = 25$  kHz) and m16 (c3, c6,  $\nu_r = 40$  kHz) phasing schemes apply-

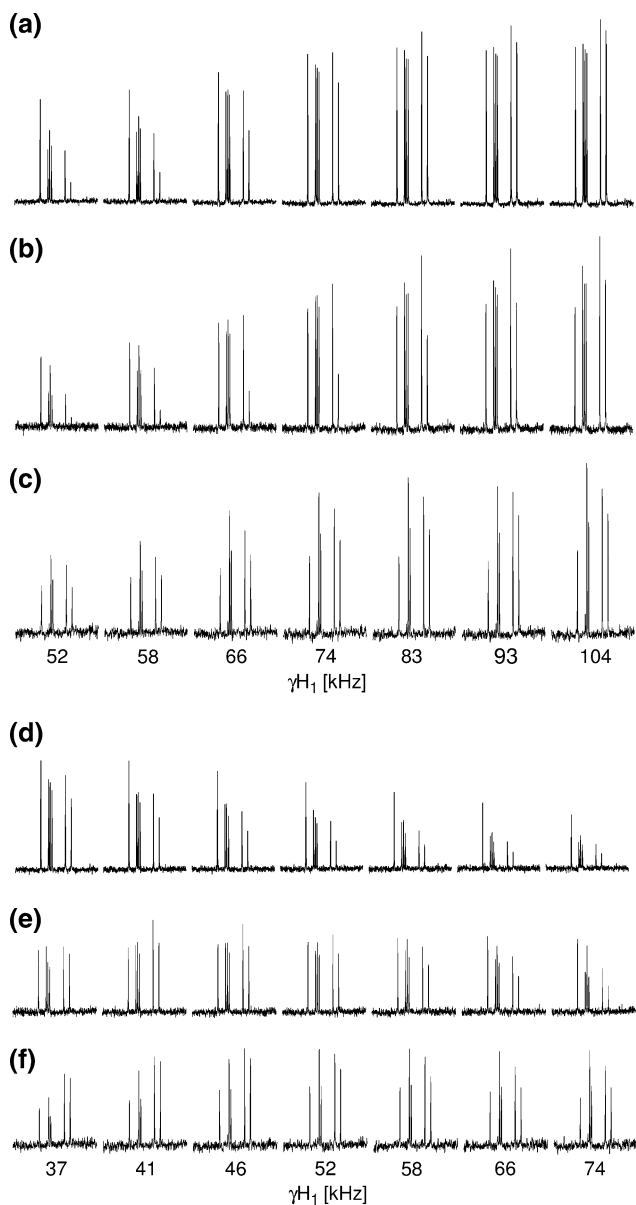


**Fig. 3** The  $^{13}\text{C}$  signal obtained with  $t_1 = 0$  and as a function of the  $^{13}\text{C}$  RF field strength applied during adiabatic mixing in different chemical shift correlation experiments carried out at a spinning speed of 25 kHz without  $^1\text{H}$  decoupling during mixing (dpwr-mix = 0) (a, b, c) and with  $^1\text{H}$  decoupling during mixing (dpwr-mix = 120 kHz) (d, e, f). The spectra were generated with an acquisition time of 10 ms, CP contact time of 350  $\mu\text{s}$  and a recycle time of 2.5 s. (a, d) single-quantum dipolar with 16 transients and mixing time of 1.92 ms with  $\text{R}6_6^2\text{R}6_6^{-2}$  symmetry-based sequence, (b, e) single-quantum scalar with 16 transients and a mixing time of 2.24 ms with  $\text{R}32_{28}^3$  symmetry-based sequence and (c, f) double-quantum dipolar correlation experiment with 64 transients and a net mixing time of 320  $\mu\text{s}$  with m4 phasing scheme

ing one pulse per rotor period. Other details are given in the figure captions. The data presented in Fig. 2 clearly suggest that a continuous train of adiabatic  $^{13}\text{C}$  inversion pulses applied at high RF field strengths leads to efficient broadband heteronuclear decoupling. This is consistent with numerical and experimental  $^{13}\text{C}$  MAS NMR studies at very high spinning speeds (Riedel et al. unpublished) which reveal that a continuous train of high power  $^1\text{H}$  tanh/tan adiabatic pulses with an inversion pulse width equal to the rotor period leads to efficient heteronuclear decoupling. This is not surprising considering the fact that the application of an  $^1\text{H}$  inversion pulse at the center of a rotor period leads to a net dipolar dephasing of the observed  $^{13}\text{C}$  magnetisation. The inversion pulse applied at the center of the subsequent rotor period results in the refocussing of this dephased magnetisation at the end of the second rotor period and hence to efficient

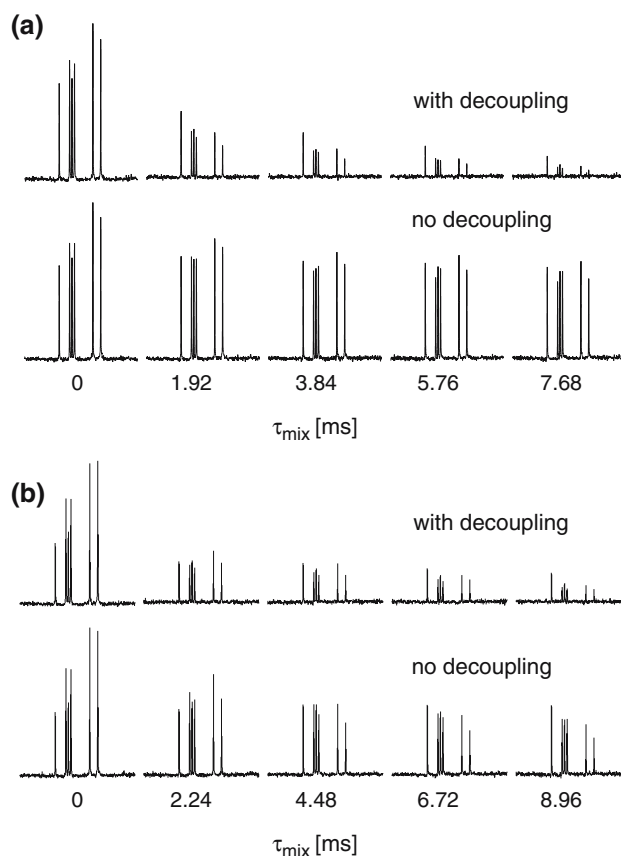
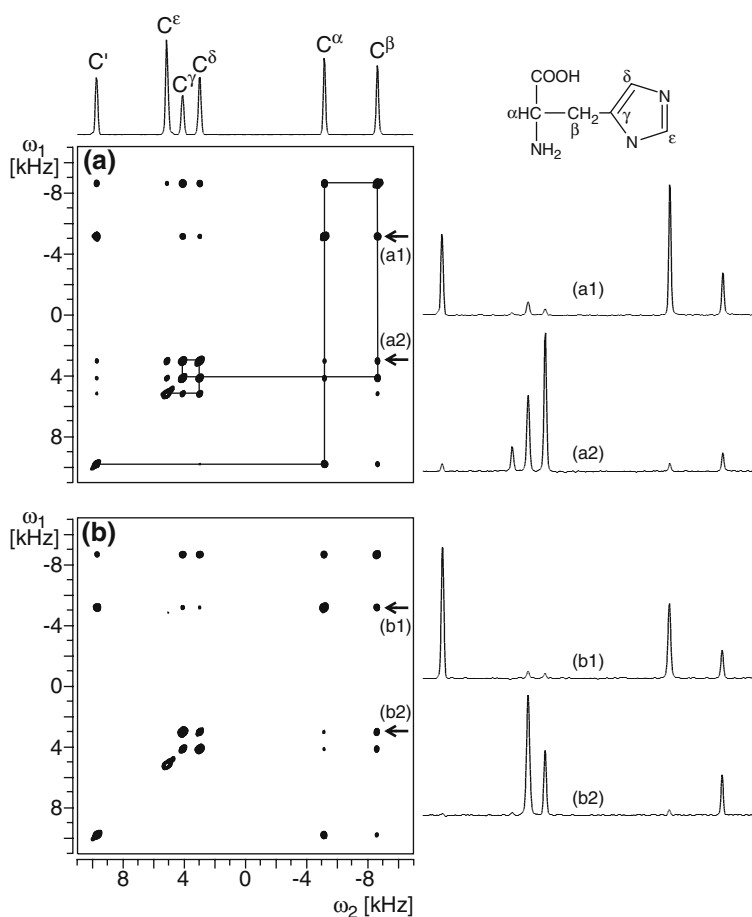


**Fig. 4** The  $^{13}\text{C}$  signal obtained as a function of the adiabatic mixing time in single-quantum dipolar (a) and single-quantum scalar coupling (b) mediated correlation experiments carried out at a spinning speed of 25 kHz with (dpwr-mix = 120 kHz) and without (dpwr-mix = 0 kHz)  $^1\text{H}$  decoupling during mixing.  $^{13}\text{C}$  RF field strengths, respectively, of 41.5 kHz and 104 kHz in (a) and 46.4 kHz and 104 kHz in (b) were employed for generating data with and without  $^1\text{H}$  decoupling. All other parameter values were as given in Fig. 3

heteronuclear decoupling. Even with mixing schemes involving the application of inversion pulses with durations not equal to the rotor period, it is seen from Fig. b1–b3 that efficient heteronuclear decoupling can be achieved if the mixing scheme employed explicitly removes heteronuclear dipolar interactions. Besides the simulations given above, a variety of other calculations were also carried out for all the cases considering, e.g. different phasing schemes or different symmetry-based mixing sequences (data not shown). Results from these studies indicate that it is possible to employ a variety of phasing schemes and obtain  $^{13}\text{C}$  RF field strength dependence similar to that shown in Fig. 2. Hence, it should be feasible to carry out chemical shift correlation experiments using adiabatic RF pulse schemes without  $^1\text{H}$  decoupling during mixing. The conclusions reached via numerical simulations have been confirmed by experimental measurements. In Fig. 3 the signal obtained with  $t_1 = 0$  in single-quantum dipolar (a, d), single-quantum scalar (b, e) and double-quantum dipolar (c, f) chemical shift correlation experiments carried out without (a, b, c) and with (d, e, f)  $^1\text{H}$  decoupling during mixing are plotted

as a function of the  $^{13}\text{C}$  adiabatic RF field strength applied. Due to hardware limitations, tanh/tan adiabatic inversion pulses of 33  $\mu\text{s}$  duration and centered at the middle of each rotor period were employed in the double-quantum experiment. Other details are given in the figure caption. As expected from numerical simulations, it is seen that the observed signal intensity in Fig. 3a–c reaches the maximum at  $\sim 100$  kHz. For the adiabatic pulse widths used in generating the plots in Fig. 3d–f the maximum signal intensity should be seen, based on our earlier studies (Leppert et al. 2003; Riedel et al. 2006a), at  $^{13}\text{C}$  RF field strengths of  $\sim 40$  kHz and  $\sim 45$ – $50$  kHz in the single-quantum dipolar and double-quantum chemical shift correlation experiments, respectively. The data presented below for scalar coupling mediated polarisation transfer suggest maximum signal intensity for a  $^{13}\text{C}$  RF field strengths of  $\sim 80$ – $100$  kHz. Additionally, above these critical threshold values the intensity of the observed signal should exhibit minimal variations. However, at the high spinning speed employed, the maximum signal intensity observed in all the three experiments (3d–3f) is much smaller than the corresponding intensity

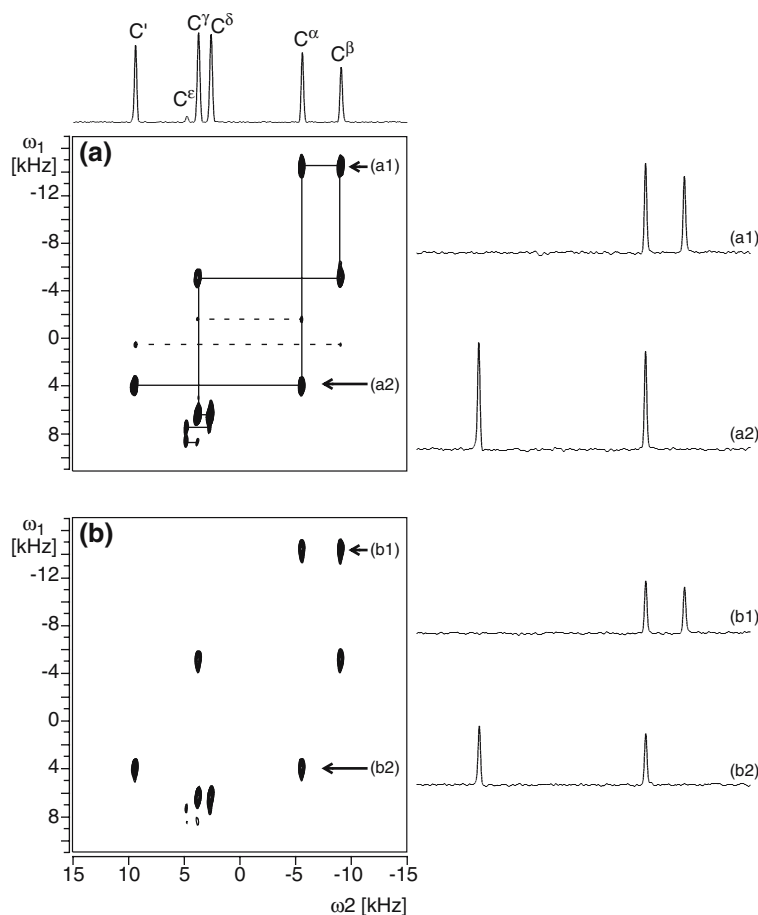
**Fig. 5** 2D  $^{13}\text{C}$  single-quantum dipolar (a) and scalar coupling (b) mediated chemical shift correlation spectra obtained at a spinning speed of 25 kHz without  $^1\text{H}$  decoupling (dpwrmix = 0 kHz) and with  $^{13}\text{C}$  RF field strength of 104 kHz during adiabatic mixing. The spectra were generated with 16 transients per  $t_1$  increment, 256  $t_1$  increments, spectral width in the indirect dimension of 50,000 Hz and recycle time of 2 s. The  $\text{R}_{6_6}^2\text{R}_{6_6}^{-2}$  symmetry-based sequence was used in the through-space experiment with a mixing time of 3.84 ms. The through-bond spectrum was generated with a mixing time of 6.72 ms and the  $\text{R}_{32_{28}}^3$  symmetry-based sequence. A few representative cross-sections are also given to indicate spectral quality



obtained without using  $^1\text{H}$  decoupling (3a–3c). Due to the interference between the recoupling and decoupling fields, the signal intensities further get diminished at higher  $^{13}\text{C}$  RF field strengths. The  $^{13}\text{C}$  signal intensities obtained for  $t_1 = 0$  and as a function of the mixing time (Fig. 4) also suggest that in situations where high  $^{13}\text{C}$  RF field strength is available it will be advantageous to carry out chemical shift correlation experiments without  $^1\text{H}$  decoupling during mixing. In Fig. 5 we present 2D single-quantum dipolar (a) and scalar (b) coupling mediated chemical shift correlation spectra recorded without applying  $^1\text{H}$  decoupling during mixing. The mixing scheme used for generating the through-bond spectrum was constructed based on well established procedures for suppressing and/or selecting the desired nuclear spin interaction terms in the lowest-order average Hamiltonian (Carravetta et al. 2000; Brinkmann and Levitt 2001; Levitt 2002). The 2D double-quantum NMR spectra obtained without (a) and with (b)  $^1\text{H}$  decoupling during mixing are given in Fig. 6. A few representative cross-sections are also given in Figs. 5 and 6. The single-quantum dipolar and scalar coupling mediated correlation data were

generated using mixing times of 3.84 and 6.72 ms, respectively. The double-quantum NMR spectra were generated using the m4 phasing scheme with  $\tau_{\text{mix}} = 320 \mu\text{s}$ . All the correlation spectra show the expected connectivities. Even for the short mixing time employed in the double-quantum experiment, the cross-sections in the spectrum collected without  $^1\text{H}$  decoupling show improved signal to noise ratio. Single-quantum correlation spectra were also collected as a function of the mixing time and the build-up of cross-peak intensities were as expected for polarisation transfer via  $^{13}\text{C}$ – $^{13}\text{C}$  dipolar and scalar couplings (data not shown). At the mixing time used, it is expected from the polarisation transfer characteristics given in Fig. 7a, b that the  $^{13}\text{C}^\alpha \rightarrow ^{13}\text{C}'$  cross-peak intensity should be much larger than that of the  $^{13}\text{C}^\alpha \rightarrow ^{13}\text{C}^\beta$  cross-peak in Fig. 5b. Although the contribution to the signal intensities arising from one bond  $^{13}\text{C}$ – $^{13}\text{C}$  dipolar couplings may not be completely eliminated, unlike the dipolar correlation spectrum, the through-bond spectra should be free of cross-peaks involving isolated carbons such as the  $^{13}\text{C}^\epsilon$  of histidine. The spectral cross-sections given in Fig. 5 are in general

**Fig. 6** 2D  $^{13}\text{C}$  double-quantum dipolar chemical shift correlation spectra obtained using the m4 phasing scheme at a spinning speed of 25 kHz without (a, dpwr-mix = 0 kHz) and with (b, dpwr-mix = 120 kHz)  $^1\text{H}$  decoupling.  $^{13}\text{C}$  RF field strengths of 104 kHz (a) and 46.4 kHz (b) were used during adiabatic mixing. The spectra were generated with 64 transients per  $t_1$  increment, 96  $t_1$  increments, spectral width in the indirect dimension of 50,000 Hz and recycle time of 2 s. A few representative cross-sections are also given to indicate spectral quality



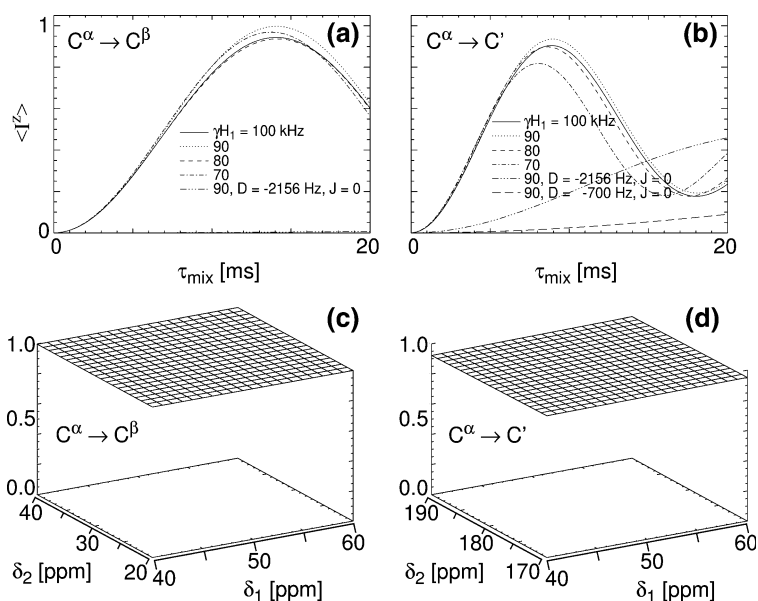


**Fig. 7** Magnetisation transfer characteristics under the  $R32_{28}^3$  symmetry-based adiabatic RF pulse scheme using tanh/tan pulses of  $35 \mu\text{s}$  duration. At a spinning speed of  $25 \text{ kHz}$  the magnitude of the transferred magnetisation (normalised to the maximum transferable signal) on the second spin ( $^{13}\text{C}^\beta/^{13}\text{C}'$ ) was monitored starting with ( $I_{1z}$ ) magnetisation on spin 1 ( $^{13}\text{C}^\alpha$ ) at zero mixing time and after adiabatic mixing. For the  $\text{C}^\alpha \rightarrow \text{C}^\beta$  and  $\text{C}^\alpha \rightarrow \text{C}'$  transfers  $^{13}\text{C}$  CS tensor, scalar and dipolar coupling parameters of alanine and glycine as in our earlier studies (Brinkmann et al. 2002; Leppert et al. 2003) were respectively used. Plots given in (a) and (b) show the dependence on the  $^{13}\text{C}$

RF field strength as a function of the adiabatic mixing time. A few representative plots generated with  $J_{\text{CC}} = 0$  are given to indicate the extent of dipolar contribution to magnetisation transfer. The  $^{13}\text{C}$  carrier frequency was kept at the center of the corresponding carbon resonances. Plots given in (c) and (d) represent the transferred signal amplitude as a function of the isotropic chemical shifts  $\delta_1$  and  $\delta_2$  of the two nuclei. These plots were generated using a  $^{13}\text{C}$  RF field strength of  $90 \text{ kHz}$  and mixing times of  $14.56 \text{ ms}$  (c) and  $8.96 \text{ ms}$  (d). The  $^{13}\text{C}$  carrier frequency was kept at  $110 \text{ ppm}$

agreement with these expectations. To further confirm that the cross-peaks in the spectra given in Fig. 5 arise due to the  $^{13}\text{C}$  adiabatic mixing schemes employed, we also acquired single-quantum chemical shift correlation spectra via the proton driven  $^{13}\text{C}$  spin diffusion approach (i.e., with no RF irradiation applied on the  $^1\text{H}$  and  $^{13}\text{C}$  channels). At the spinning speed of  $25 \text{ kHz}$ , cross-peaks with measurable intensities could be seen only between  $\text{C}^\alpha$  and  $\text{C}^\beta$  carbons and  $\text{C}^\gamma$  and  $\text{C}^\delta$  carbons for different short mixing times (data not shown). This provides further evidence that although the spectra shown in Fig. 5 were collected without  $^1\text{H}$  decoupling during mixing, the cross-peaks in these spectra mainly originate due to the  $^{13}\text{C}$  adiabatic mixing scheme employed for achieving chemical shift correlation via  $^{13}\text{C}$ – $^{13}\text{C}$  dipolar (a) and scalar (b) couplings. It is worth mentioning here that the potential of symmetry-based adiabatic mixing schemes, with  $^1\text{H}$  decoupling during mixing, has been recently demonstrated for generating through-bond chemical shift correlation spectra at very high spinning speeds (Hardy et al. 2003). While the success of the approach of Hardy et al. (2003) is critically dependent on the strength

of the  $^1\text{H}$  decoupling RF field strength used during mixing, the method presented here can be conveniently carried out without  $^1\text{H}$  decoupling. While we have presented in our earlier studies numerical simulations to clearly demonstrate the potential of tanh/tan adiabatic mixing schemes for generating broadband dipolar chemical shift correlation spectra (Leppert et al. 2003; Riedel et al. 2006a), the numerical simulations shown in Fig. 7c, d illustrate that adiabatic symmetry-based mixing schemes such as  $R32_{28}^3$  can be effectively employed for generating broadband through-bond correlation spectra. In conclusion, it has been demonstrated that at high spinning speeds it is possible to generate broadband  $^{13}\text{C}$  chemical shift correlation data without  $^1\text{H}$  decoupling during adiabatic mixing and such an approach will be the method of choice in situations where large  $^{13}\text{C}$  RF field strength is available.

**Acknowledgements** This study has been funded in part by a PhD fellowship to Kerstin Riedel from Stiftung Stipendien-Fonds des Verbandes der Chemischen Industrie e.V. The FLI is a member of the Science Association ‘Gottfried Wilhelm Leibniz’ (WGL) and is financially supported by the Federal Government of Germany and the State of Thuringia.



## References

- Bak M, Nielsen NC (1997) REPULSION, A novel approach to efficient powder averaging in solid-state NMR. *J Magn Reson* 125:132–139
- Bak M, Rasmussen JT, Nielsen NC (2000) SIMPSON: a general simulation program for solid-state NMR spectroscopy. *J Magn Reson* 147:296–330
- Baldus M (2002) Correlation experiments for assignment and structure elucidation of immobilized polypeptides under magic angle spinning. *Prog Nucl Magn Reson Spectrosc* 41:1–47
- Bennett AE, Griffin RG, Vega S (1994) Recoupling of homo- and heteronuclear dipolar interactions in rotating solids. In: *NMR basic principles and progress*, vol 33. Springer, Berlin, pp 1–77
- Bennett AE, Rienstra CM, Auger M, Lakshmi KV, Griffin RG (1995) Heteronuclear decoupling in rotating solids. *J Chem Phys* 103:6951–6958
- Bennett AE, Rienstra CM, Griffiths JM, Zhen W, Lansbury PT, Griffin RG (1998) Homonuclear radio frequency-driven recoupling in rotating solids. *J Chem Phys* 108:9463–9479
- Brinkmann A, Levitt MH (2001) Symmetry principles in the nuclear magnetic resonance of spinning solids: heteronuclear recoupling by generalized Hartmann-Hahn sequences. *J Chem Phys* 115:357–384
- Brinkmann A, Schmedt auf der Günne J, Levitt MH (2002) Homonuclear zero-quantum recoupling in fast magic-angle spinning nuclear magnetic resonance. *J Magn Reson* 156:79–96
- Carravetta M, Eden M, Zhao X, Brinkmann A, Levitt MH (2000) Symmetry principles for the design of radiofrequency pulse sequences in the nuclear magnetic resonance of rotating solids. *Chem Phys Lett* 321:205–215
- De Paepe G, Bayro MJ, Lewandowski J, Griffin RG (2006) Broadband homonuclear correlation spectroscopy at high magnetic fields and MAS frequencies. *J Am Chem Soc* 128:1776–1777
- Dusold S, Sebald A (2000) Dipolar recoupling under magic-angle spinning conditions. *Annu Rep NMR Spectrosc* 41:185–264
- Griffin RG (1998) Dipolar recoupling in MAS spectra of biological solids. *Nature Struct Biol* 5:508–512
- Hardy EH, Detken A, Meier BH (2003) Fast-MAS total through-bond correlation spectroscopy using adiabatic pulses. *J Magn Reson* 165:208–218
- Heise B, Leppert J, Ohlenschläger O, Görlach M, Ramachandran R (2002) Chemical shift correlation via RFDR: elimination of resonance offset effects. *J Biomol NMR* 24:237–243
- Herbst C (2006a) Festkörper-NMR-Untersuchungen an isotoopen-markierten biologischen Systemen, Diploma, Friedrich-Schiller-Universität Jena
- Herbst C, Riedel K, Leppert J, Ohlenschläger O, Görlach M, Ramachandran R (2006b) Solid state NMR at high magic angle spinning frequencies: dipolar chemical shift correlation with adiabatic inversion pulse based RF pulse schemes. *J Biomol NMR* 35:241–248
- Hughes CE, Luca S, Baldus M (2004) Radio-frequency driven polarization transfer without heteronuclear decoupling in rotating solids. *Chem Phys Lett* 385:435–440
- Hwang TL, van Zijl PCM, Garwood M (1998) Fast broadband inversion by adiabatic pulses. *J Magn Reson* 133:200–203
- Leppert J, Heise B, Görlach M, Ramachandran R (2002) REDOR: an assessment of the efficacy of dipolar recoupling with adiabatic inversion pulses. *J Biomol NMR* 23:227–238
- Leppert J, Heise B, Ohlenschläger O, Görlach M, Ramachandran R (2003) Broadband RFDR with adiabatic inversion pulses. *J Biomol NMR* 26:13–24
- Leppert J, Ohlenschläger O, Görlach M, Ramachandran R (2004a) Adiabatic TOBSY in rotating solids. *J Biomol NMR* 29:167–173
- Leppert J, Urbinati CR, Häfner S, Ohlenschläger O, Swanson MS, Görlach M, Ramachandran R (2004b) Identification of NH...N hydrogen bonds by magic angle spinning solid state NMR in a double-stranded RNA associated with myotonic dystrophy. *Nucleic Acids Res* 31:1177–1183
- Leppert J, Ohlenschläger O, Görlach M, Ramachandran R (2004c) RFDR with adiabatic inversion pulses: application to internuclear distance measurements. *J Biomol NMR* 28:229–233
- Leppert J, Ohlenschläger O, Görlach M, Ramachandran R (2004d) Adiabatic heteronuclear decoupling in rotating solids. *J Biomol NMR* 29:319–324
- Levitt MH, Freeman R, Frenkiel T (1983) Broadband decoupling in high-resolution nuclear magnetic resonance spectroscopy. *Adv Magn Reson* 11:47–110
- Levitt MH (2002) Symmetry-based pulse sequences in magic-angle spinning solid-state NMR. In: Grant DM, Harris RK (eds) *Encyclopedia of nuclear magnetic resonance*, vol 9. John Wiley, Chichester, New York, p 165
- Marin-Montesinos I, Brouwer DH, Antonioli G, Lai WC, Brinkmann A, Levitt MH (2005) Heteronuclear decoupling interference during symmetry-based homonuclear recoupling in solid-state NMR. *J Magn Reson* 177:307–317
- McDermott AE (2004) Structural and dynamic studies of proteins by solid-state NMR spectroscopy: rapid movement forward. *Curr Opin Struct Biol* 14:554–561
- Mou Y, Chao JCH, Chan JCC (2006) Efficient spin-spin scalar coupling mediated C-13 homonuclear polarization transfer in biological solids without proton decoupling. *Solid State Nucl Magn Reson* 29:278–282
- Riedel K (2004) Festkörper-NMR untersuchungen von ribonukleinsäuren mittels adiabatischer symmetriebasierter pulssequenzen, Diploma, Friedrich-Schiller-Universität Jena
- Riedel K, Leppert J, Ohlenschläger O, Görlach M, Ramachandran R (2004a) Heteronuclear decoupling in rotating solids via symmetry-based adiabatic RF pulse schemes. *Chem Phys Lett* 395:356–361
- Riedel K, Leppert J, Häfner S, Ohlenschläger O, Görlach M, Ramachandran R (2004b) Homonuclear chemical shift correlation in rotating solids via  $RN_n^v$  symmetry-based adiabatic RF pulse schemes. *J Biomol NMR* 30:389–395
- Riedel K, Leppert J, Ohlenschläger O, Görlach M, Ramachandran R (2005) TEDOR with adiabatic inversion pulses: resonance assignments of  $^{13}C/^{15}N$  labelled RNAs. *J Biomol NMR* 31:49–57
- Riedel K, Herbst C, Leppert J, Ohlenschläger O, Görlach M, Ramachandran R (2006a) Broadband homonuclear double-quantum NMR/filtering via zero-quantum dipolar recoupling in rotating solids. *Chem Phys Lett* 424:178–183

- Riedel K, Herbst C, Leppert J, Ohlenschläger O, Görlach M, Ramachandran R (2006b) Tailoring broadband inversion pulses for MAS solid state NMR. *J Biomol NMR* 35:275–283
- Riedel K, Herbst C, Leppert J, Ohlenschläger O, Görlach M, Ramachandran R (2006c) Heteronuclear decoupling in rotating solids: improving the efficacy of  $CN_n^y$  symmetry-based tanh/tan adiabatic RF pulse schemes. *Chem Phys Lett* 429:590–594
- States DJ, Haberkorn RA, Ruben DJ (1982) A two-dimensional nuclear overhauser experiment with pure absorption phase in four quadrants. *J Magn Reson* 48:286–292
- Thompson LK (2002) Solid-state NMR studies of the structure and mechanisms of proteins. *Curr Opin Struct Biol* 12:661–669